Polarized radiative transfer

Light + matter + magnetic field

Nikolai Piskunov
Uppsala University

What happen to absorption in magnetic field?

- Projection of electron orbital momentum on magnetic field is quantised M=-J,0,+J
- Calssical analogy: electron oscillates along field direction (M=0) or circles around it (M=-1,+1).
- Allowed transitions can change M by 0 or 1.
- Photon can carry angular momentum in form of circular polarization

Equations of radiative transfer

- Now we are going to treat separately photons that carry angular momentum (circularly polarised light) and that do not (linearly polarised light)

- For each of these we can write a separate RT equation:

$$\frac{dI^p}{dx} = -\left\{K^p_{\parallel}, K^p_{\perp}, K^p_{\circlearrowleft}, K^p_{\circlearrowright}\right\} \cdot \left\{\begin{array}{c} I^{\parallel} \\ I^{\perp} \\ I^{\circlearrowleft} \\ I^{\circlearrowright} \end{array}\right\} + J^p$$

Stokes parameters and RT equation

- The previous equation was written for one particular corrdinate system with x pointing to the propagation of light and y,z selected arbitrarily in the perpendicular plane
- It tuns out that we can reduce this uncertainty by adding and subtracting the equations for circular polarization and for linear polarisation $I = I^{\perp} + I^{\parallel} + I^{\circlearrowleft} + I^{\circlearrowright}$
- In this case we will only need two angles in y,z-plane
- Addition gives us total intensity
- Subtraction will give us circular ($I^{\circlearrowleft} - I^{\circlearrowright} \equiv V$) and two linear ($I^{\parallel} - I^{\perp} \equiv Q$ and U) polarisations

Canonical polarized RTE

- The form of RT equation for Stokes parameters looks like this:

$$\frac{d\vec{I}}{dx} = -\mathbb{K} \cdot \vec{I} + \vec{J}$$

- Where: $\vec{I} = \{I, Q, U, V\}$ are the Stokes parameters

$$\mathbb{K} = \begin{pmatrix} \eta_I & \eta_Q & \eta_U & \eta_V \\ \eta_Q & \eta_I & \rho_V & -\rho_U \\ \eta_U & -\rho_V & \eta_I & \rho_Q \\ \eta_V & \rho_U & -\rho_Q & \eta_I \end{pmatrix}$$

Final touches

- We can make a simple trick at the diagonal of the "absorption matrix":

$$\tilde{\mathbb{K}} = \frac{\mathbb{K}}{\eta_I} - 1$$

- The new matrix has zeros on main diagonal

- The source function in unstructured medium is defined as: $\vec{S} = \vec{J}/\eta_I$

Final-final touches

- Now the next final form of the RT equation:

$$\frac{d\vec{I}}{dx} = -\eta_I \tilde{\mathbb{K}} \cdot \vec{I} - \eta_I \vec{I} + \eta_I \vec{S}$$

- We can also introduce a modified source function: $\vec{\mathfrak{S}} = \vec{S} - \tilde{\mathbb{K}}\vec{I}$

- ... and get the final form of RTE:

$$\frac{d\vec{I}}{\eta_I dx} \equiv \frac{d\vec{I}}{d\tau} = -\vec{I} + \vec{\mathfrak{S}}$$

Under the hood

Opacity matrix components:

$$
\begin{aligned}
\eta_I &= 1/2[\phi_p \sin^2\gamma + 1/2(\phi_r + \phi_b)(1 + \cos^2\gamma)] \\
\eta_Q &= 1/2[\phi_p - 1/2(\phi_r + \phi_b)\sin^2\gamma \cos 2\chi] \\
\eta_U &= 1/2[\phi_p - 1/2(\phi_r + \phi_b)\sin^2\gamma \sin 2\chi] \\
\eta_V &= 1/2(\phi_r - \phi_b)\cos\gamma \\
\rho_Q &= 1/2[\psi_p - 1/2(\psi_r + \psi_b)\sin^2\gamma \cos 2\chi] \\
\rho_U &= 1/2[\psi_p - 1/2(\psi_r + \psi_b)\sin^2\gamma \sin 2\chi] \\
\rho_V &= 1/2(\psi_r - \psi_b)\cos\gamma
\end{aligned}
$$

Opacity profiles

- Adding all sigma and all pi component profiles:

$$
\begin{aligned}
\phi_b &= \sum_b A_b H(a, v - \Delta\lambda_b/\Delta\lambda_{Dop}) \\
\phi_p &= \sum_p A_p H(a, v - \Delta\lambda_p/\Delta\lambda_{Dop}) \\
\phi_r &= \sum_r A_r H(a, v - \Delta\lambda_r/\Delta\lambda_{Dop}) \\
\psi_b &= 2\sum_b A_b F(a, v - \Delta\lambda_b/\Delta\lambda_{Dop}) \\
\psi_p &= 2\sum_p A_p F(a, v - \Delta\lambda_p/\Delta\lambda_{Dop}) \\
\psi_r &= 2\sum_r A_r F(a, v - \Delta\lambda_r/\Delta\lambda_{Dop})
\end{aligned}
$$

- The Voigt and Faradey-Voigt functions:

$$
\begin{aligned}
H(a, v) &= \frac{a}{\pi} \int_{-\infty}^{+\infty} \frac{e^{-y^2}}{(v-y)^2 + a^2} dy \\
F(a, v) &= \frac{1}{2\pi} \int_{-\infty}^{+\infty} \frac{(v-y)e^{-y^2}}{(v-y)^2 + a^2} dy
\end{aligned}
$$

Numerical solvers for polarised RTE

- Runge-Kutta, high-order, precision control on every step but slow
- Feautrier: 2nd order finite difference scheme, helps when mean intensity is needed, fast but need to cover the whole domain (long characteristics)
- Attenuation operator: fastest, 2nd order, short characteristics (one step at a time), overshooting can be handled by Bezier spline fit for the source function

Measuring Stokes parameters

- Polarizing beam-splitter

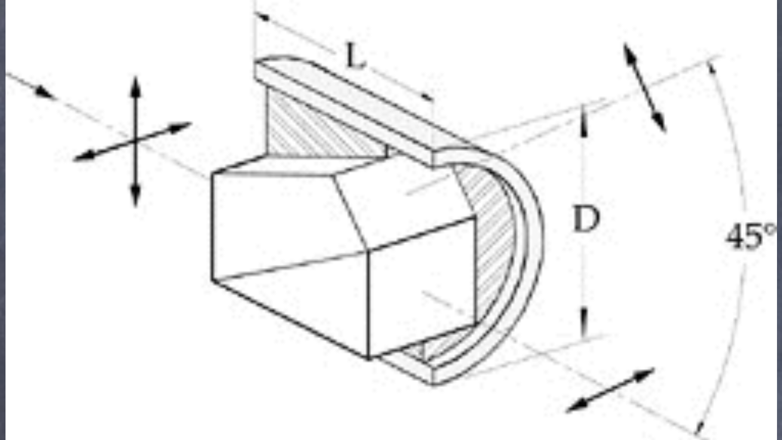

Linearly-polarized light is split in two beams

- Circular polarisation needs to be converted to linear first

A quarter-wavelength retarder plate does the trick

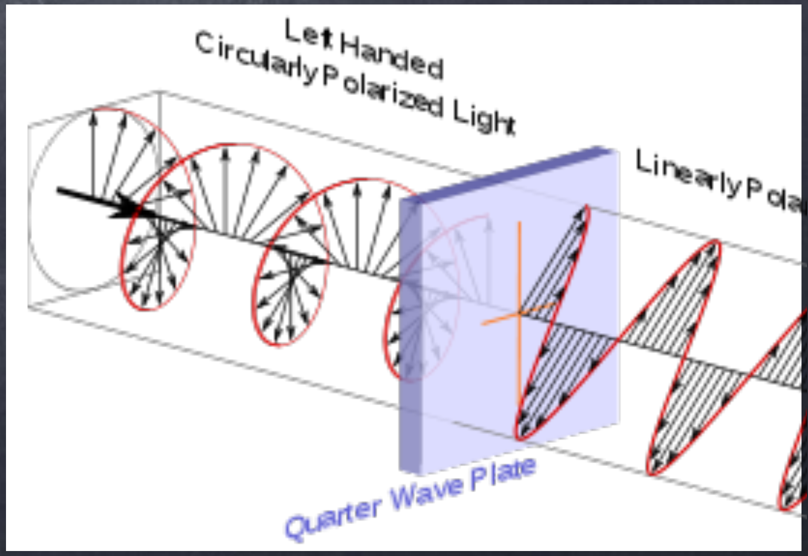

Примеры спектрополяриметрических наблюдений в 4-х параметрах Стокса *I,V,Q,U* и их анализа.
(Наблюдения проводятся для набора фаз вращения звезды)

Доплер-Зеемановское картирование магнитного поля и содержания химических элементов на поверхности звезды по наблюдениям в 4-х параметрах Стокса.

Магнитная химически-пекулярная звезда HD 24712

(Rusomarov et al. 2015, A&A 573, A123)

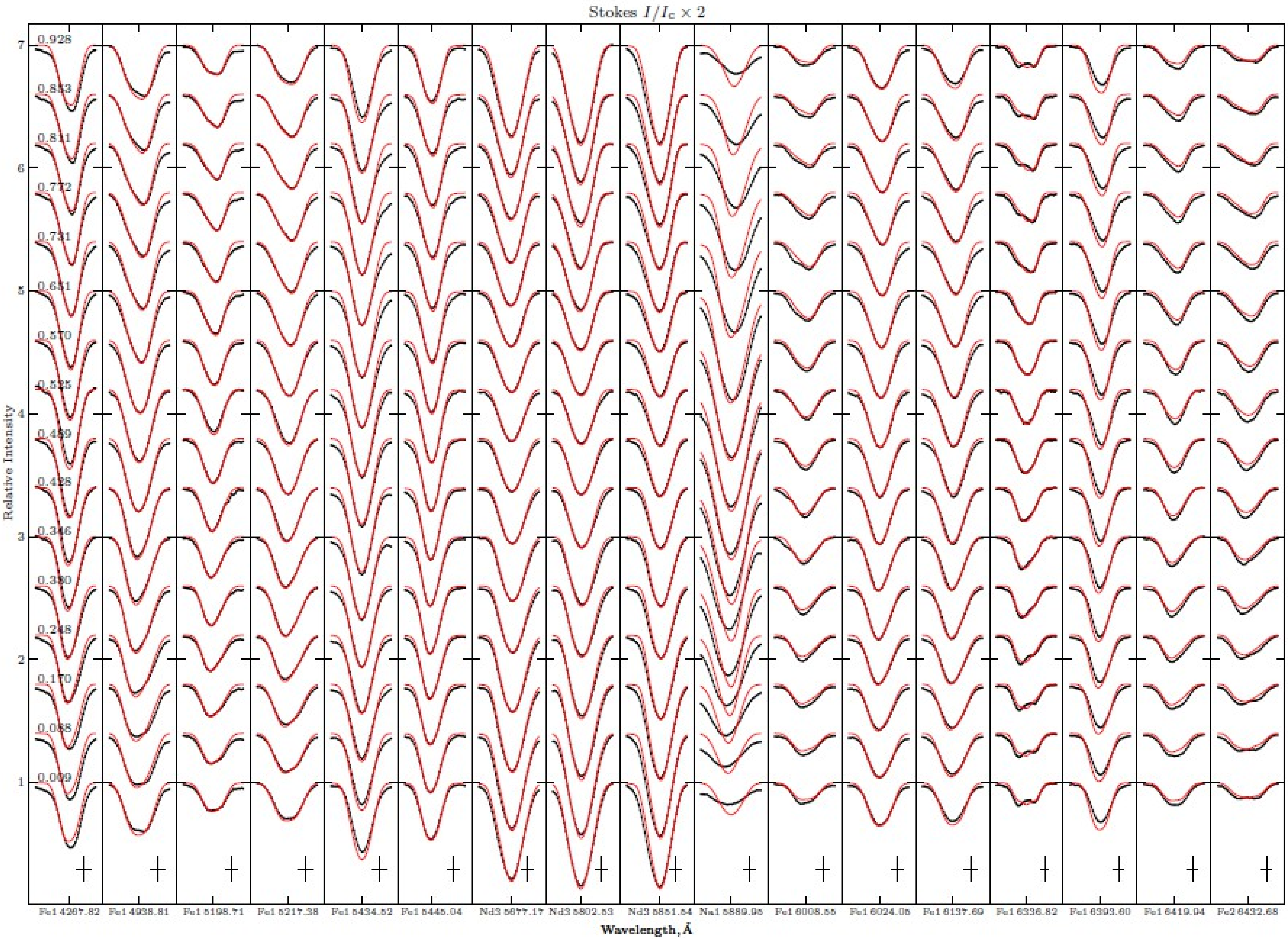

Fig. 8. Comparison of the observed (*dots*) and synthetic (*lines*) Stokes *I* profiles calculated for the final magnetic field and abundance maps (Fig. 7 and 6) for all lines (Table 1) used in the MDI inversion. The profiles have been expanded by factor 2 for clarity. The bars at the lower right of each panel show the vertical (10%) and horizontal (0.1 Å) scale. Rotational phases are indicated in the leftmost panel of the figure.

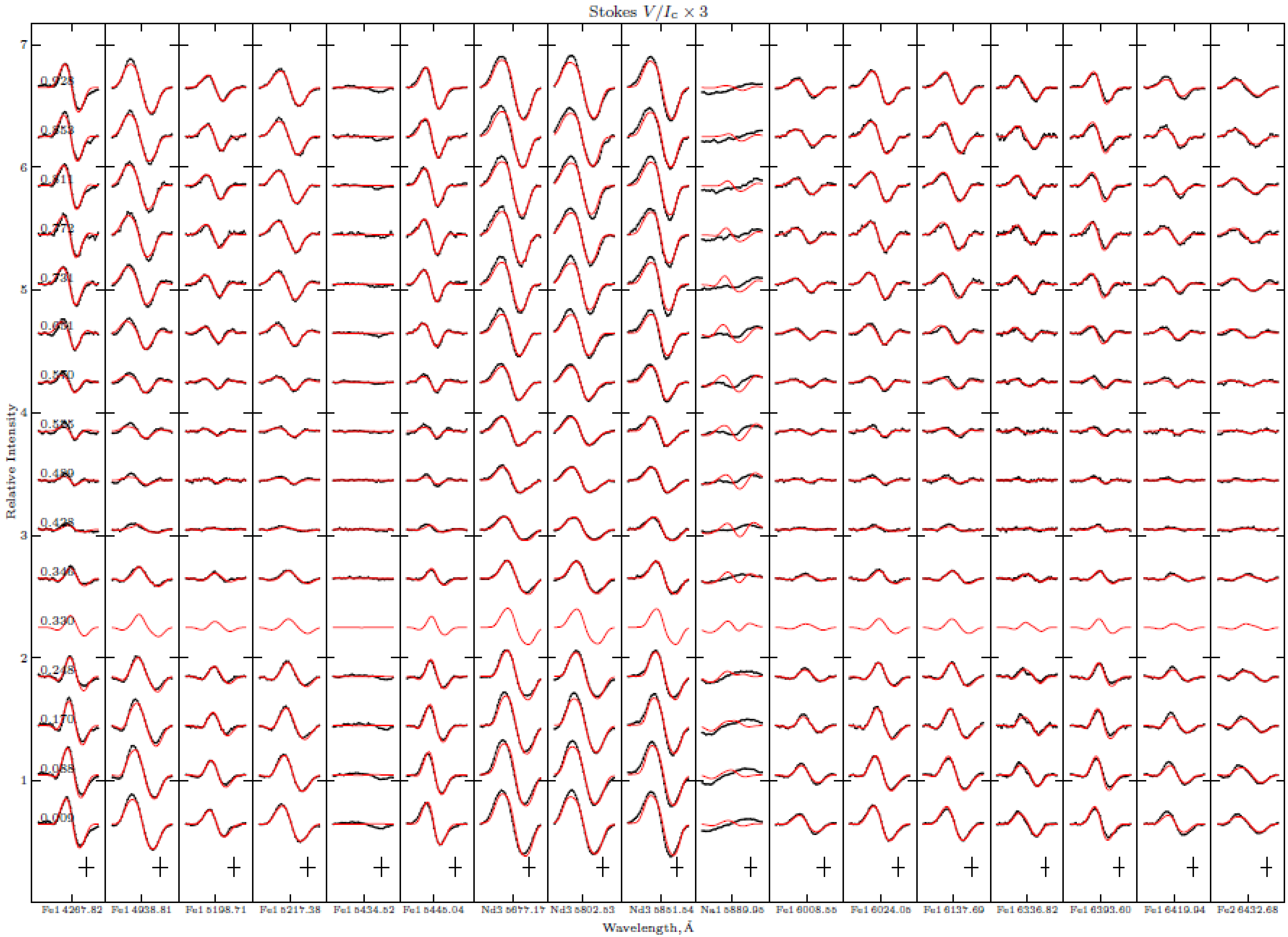

Fig. 11. Same as Fig. 8 for the Stokes V profiles. The bars at the lower right of each panel show the vertical (5%) and horizontal (0.1 Å) scale. Profiles have been rescaled by factor 3 for clarity.

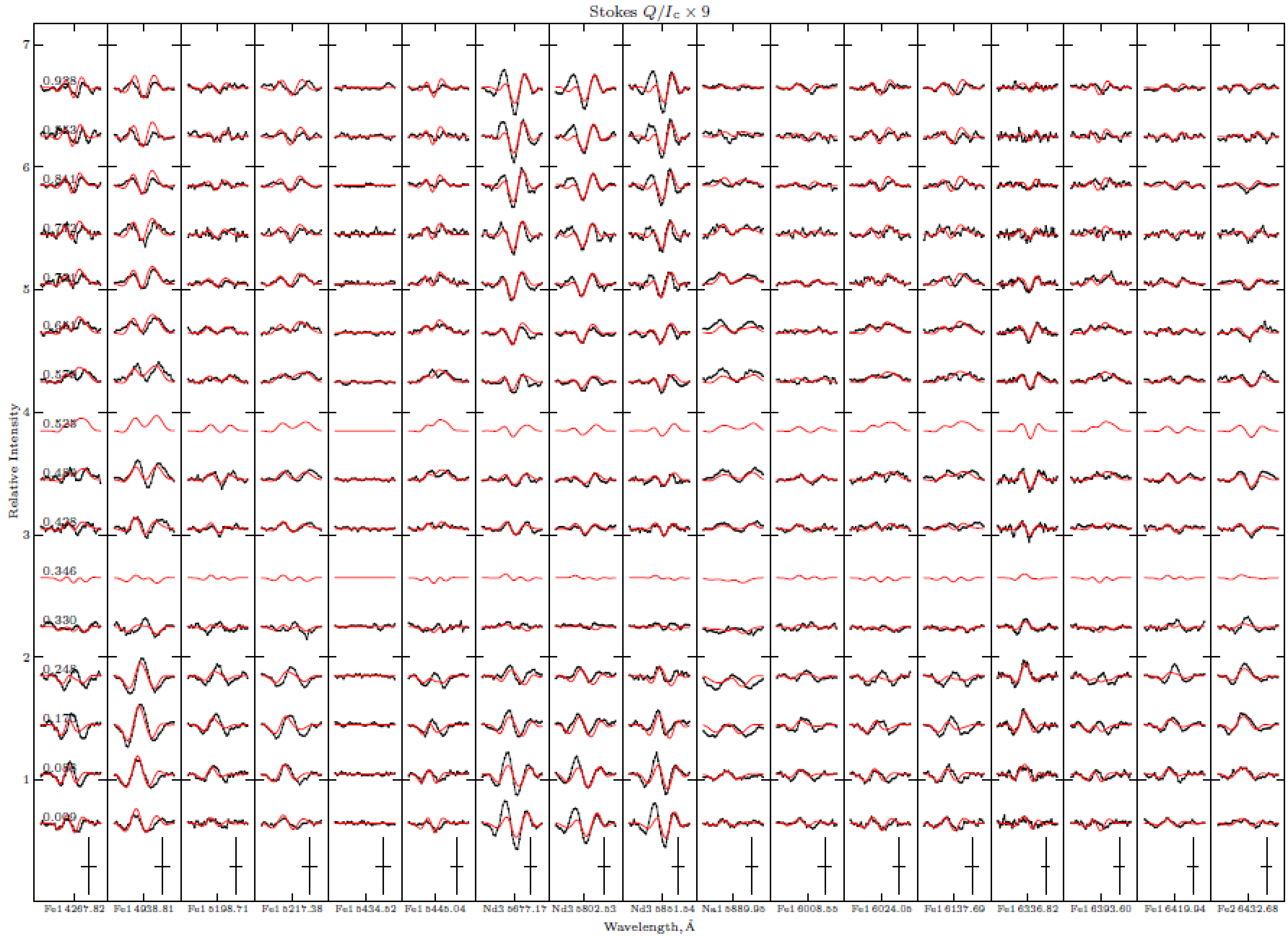

Fig. 9. Same as Fig. 8 for the Stokes Q profiles. The bars at the lower right of each panel show the vertical (5%) and horizontal (0.1 Å) scale. Profiles have been rescaled by factor 9 for clarity.

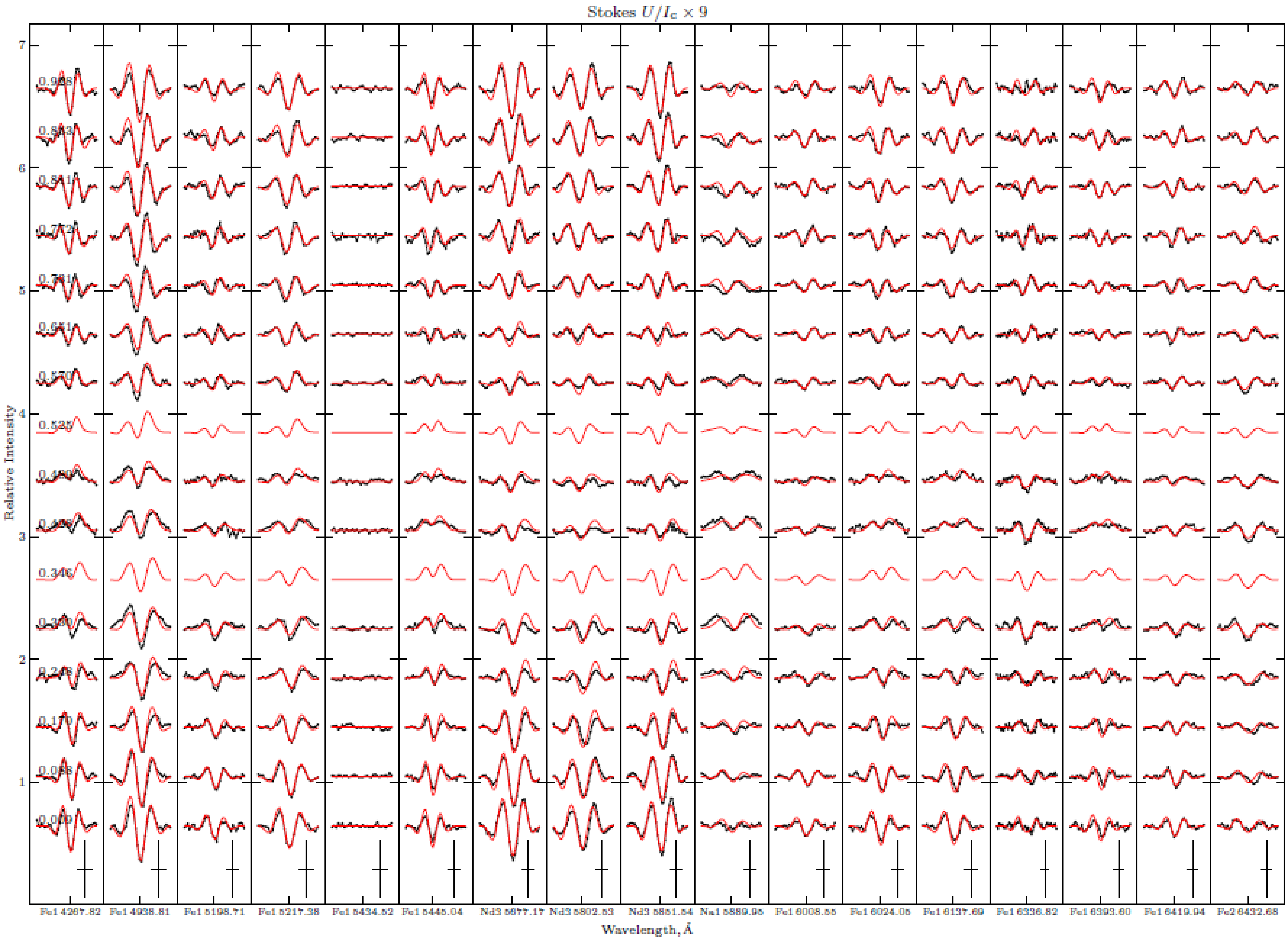

Fig. 10. Same as Fig. 8 for the Stokes U profiles. The bars at the lower right of each panel show the vertical (5%) and horizontal (0.1 Å) scale. Profiles have been rescaled by factor 9 for clarity.

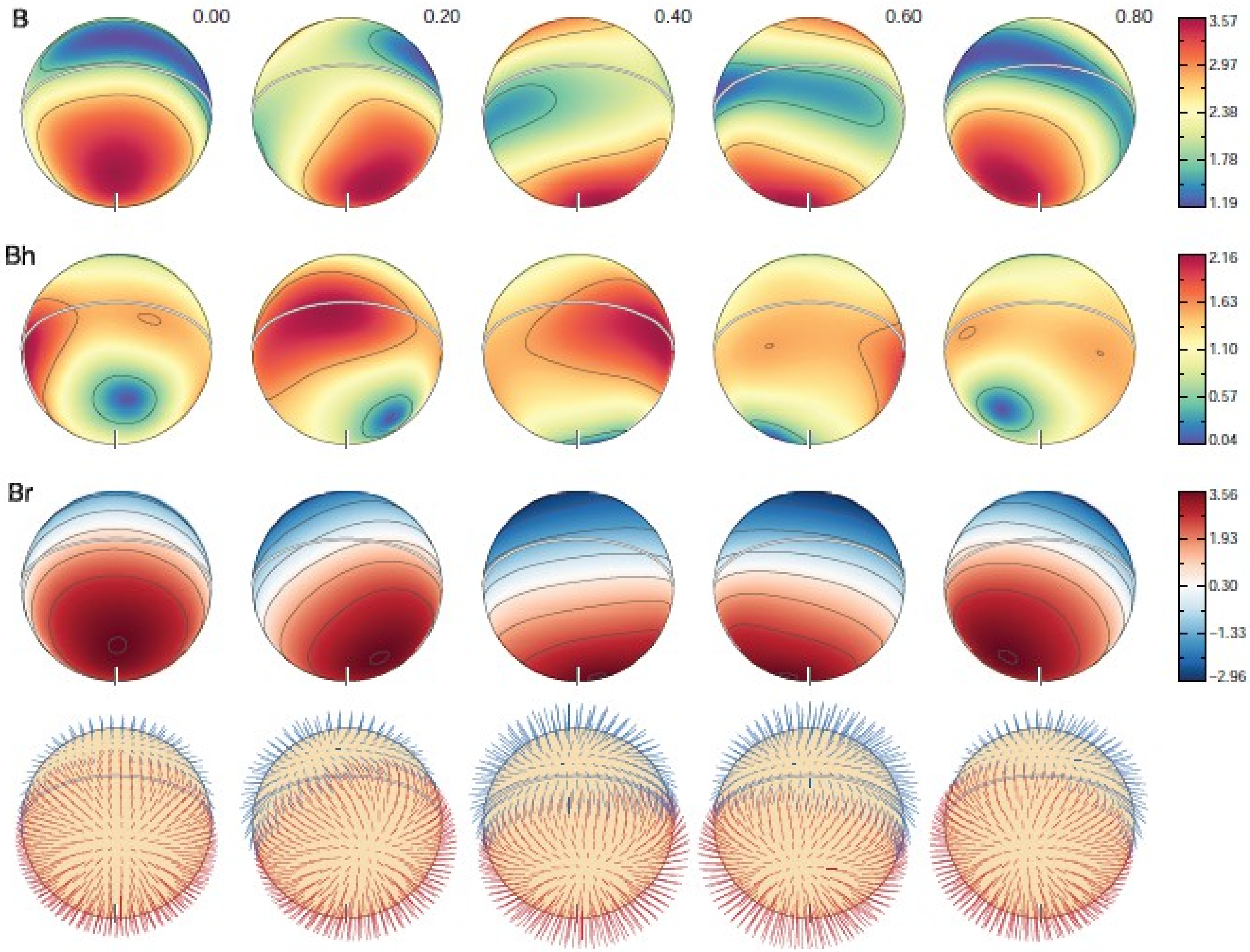

Fig. 6. Distribution of the magnetic field on the surface of HD 24712 derived from simultaneous MDI analysis of Fe, Nd III, and Na. The plots show the distribution of magnetic field modulus (*first row*), horizontal field (*second row*), radial field (*third row*), and field orientation (*fourth row*) on the surface of HD 24712. The bars on the far right represent field strength measured in kG. The contours show 1 kG changes of the according quantity. The arrow length is proportional to the field strength. The star is shown at five rotational phases, indicated above the spherical plots.

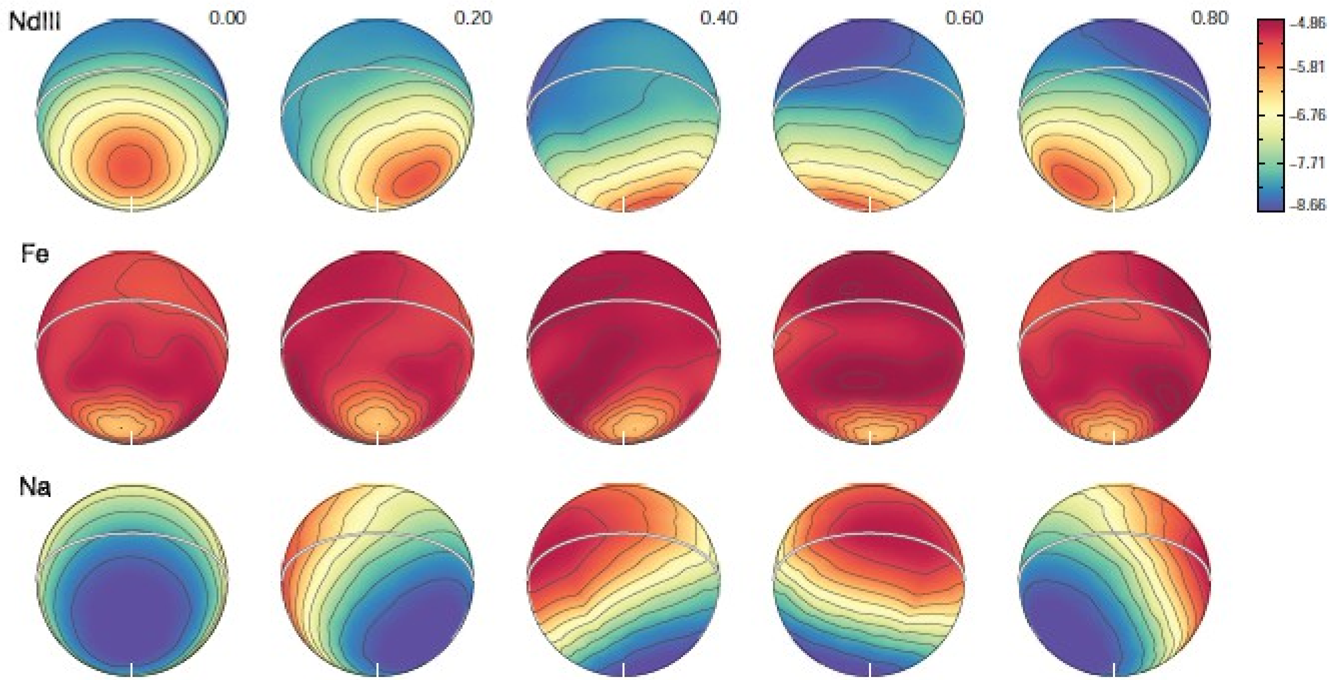

Fig. 7. Abundance distribution of Nd III, Fe, and Na on the surface of HD 24712. The *first* row shows the surface map of the Nd III, the *second* and *third* rows illustrate the surface abundance maps of Fe and Na respectively. These maps were derived from the *simultaneous* mapping of the three elements. The bars on the far right next to each panel denote the abundance in $\log(N_X/N_{\rm tot})$ units of element X. The contours for Nd III and Na are plotted with a step of 0.4 dex, and 0.2 dex for Fe. The vertical bar on each projection indicates the rotation axis.